
doi: 10.15407/ujpe63.01.0033

O.G. TRUBAIEVA,¹ A.I. LALAYANTS,¹ M.A. CHAIKA²

¹Institute for Scintillation Materials, Nat. Acad. of Sci. of Ukraine
(60, Nauky Ave., Kharkiv 61072, Ukraine; e-mail: trubaeva.olya@gmail.com)

²Institute for Single Crystals, Nat. Acad. of Sci. of Ukraine
(60, Nauky Ave., Kharkiv 61072, Ukraine; e-mail: chaika@ifpan.edu.pl)

BAND GAP CHANGE OF BULK $\text{ZnS}_x\text{Se}_{1-x}$ SEMICONDUCTORS BY CONTROLLING THE SULFUR CONTENT

ZnS_xSe_{1-x} bulk crystals were grown by the Bridgman–Stockbarger method. The transmittance of different samples in the range from 67% to 56% at $\lambda = 1100$ nm (for 4-mm samples) indicates a high optical quality of the crystals. No new states were revealed at the sulfur incorporation, and the band gap depends on the composition. The optical band gap of ZnS_xSe_{1-x} bulk crystals varies from 2.59 to 2.78 eV for direct transitions and from 2.49 to 2.70 eV for indirect transitions.

Keywords: ZnS_xSe_{1-x} bulk crystals, direct transitions, indirect transitions, band gap.

1. Introduction

In recent years, a lot of attention was focused on x-ray and γ -ray detectors based on II–VI semiconductors [1]. The band gap of such semiconductors is an important parameter, which affects the energy resolution, ionization energy, dark current, and other scintillation characteristics. The first ZnSe-based x-ray and γ -ray detectors were developed in the 1960s, and, nowadays, the detectors are mainly based on ZnSe(Te) and ZnSe(Al) [2].

As compared to ZnSe, ZnS_xSe_{1-x} semiconductors have wider band gap allowing to get better scintillation characteristics for ZnS_xSe_{1-x}-based detectors. The higher difference between atomic numbers of Zn and S as compared to Zn and Se extends the spectral range of ZnS_xSe_{1-x}-based detectors to the high-energy region. ZnS_xSe_{1-x} crystals can be grown by the molecular beam epitaxy [3, 4], hot-wall epitaxy [5], atomic layer epitaxy [6], metalorganic atomic layer epitaxy [7], metalorganic vapour phase epitaxy

[8], and laser ablation [9]. But these techniques do not allow one to fabricate large ZnS_xSe_{1-x} crystals required for x-ray and γ -ray detectors. Large ZnS_xSe_{1-x} crystals can be grown by the directional solidification techniques [10–14]. Up to now, few publications were devoted to the growth of ZnS_xSe_{1-x} bulk crystals [10–14] and growing a massive ZnS_xSe_{1-x} crystal with required properties is still a challenge.

A variation of the sulfur content in ZnS_xSe_{1-x} bulk crystals changes the growth conditions and can lead to the appearance of different defects or can change the type of chemical bonds, which, in turn, influences the width of the optical band gap [15, 16]. Accordingly, many papers report on a wide range of ZnSe band gaps between 2.25 eV [17] and 3.23 eV [18]. However, the dependence of the optical band gap width on the sulfur content in ZnS_xSe_{1-x} bulk crystals grown by the directional solidification technique still presents a gap in the study.

The possibility of a optical band gap variation by controlling the sulfur content for ZnS_xSe_{1-x} bulk crystals is discussed in this paper.

© O.G. TRUBAIEVA, A.I. LALAYANTS,
M.A. CHAIKA, 2018

ISSN 2071-0194. Ukr. J. Phys. 2018. Vol. 63, No. 1

2. Experimental

ZnS_xSe_{1-x} crystals were grown from the pre-sintered charge with $x = 0.05, 0.1, 0.15, 0.2, 0.25,$ and 0.3 . Before the growth, the raw materials were annealed in a quartz crucible at 1170 K during 5 h in the hydrogen atmosphere to remove oxygen impurities. The crystals were grown by Bridgman–Stockbarger method in the graphite crucibles with the diameter of 25 mm in the Ar atmosphere ($P_{Ar} = 2 \times 10^6$ Pa), the crystallization rate was equal to 7 mm/h, the heater temperature was in the range from 1870 to 2000 K depending on the composition of the initial raw materials. More details are described in Ref. [10, 11]. After the growth, the chemical analysis was carried out in order to determine the content of cationic impurities, as well as an actual composition of the crystal. As a result, six different compounds were obtained with the following compositions: ZnS_{0.07}Se_{0.93}; ZnS_{0.15}Se_{0.85}; ZnS_{0.22}Se_{0.78}; ZnS_{0.28}Se_{0.72}; ZnS_{0.32}Se_{0.68}; ZnS_{0.39}Se_{0.61}. The samples were annealed in zinc vapor ($T = 1223$ K, $P_{Zn} = 5 \times 10^7$ Pa, $t = 48$ h) for the final formation of luminescent centers, as well as the suppression of nonradiative relaxation channels [10, 11].

The linear optical transmission spectra of the ZnS_xSe_{1-x} bulk crystals were measured by a Shimadzu UVmini-1240 spectrophotometer in the range of 200–1100 nm. The linear optical loss coefficient was calculated according to the Lambert–Beer law taking the Fresnel reflection from the sample–air interface

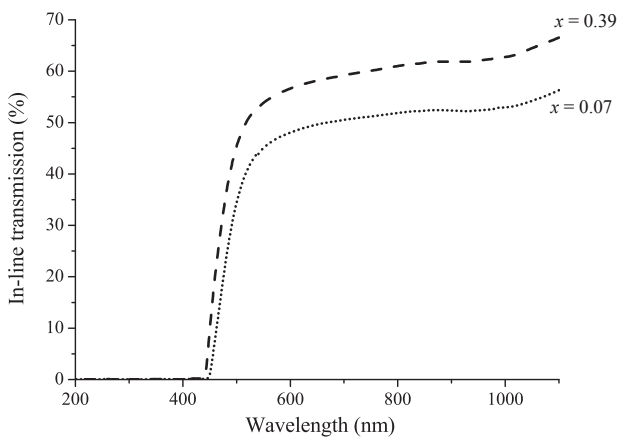


Fig. 1. Optical in-line transmission for ZnS_{0.39}Se_{0.61} (a) and ZnS_{0.07}Se_{0.93} (b) crystals

into account:

$$a = \frac{1}{h} \ln T, \quad R = \left[\frac{n_2 - n_1}{n_2 + n_1} \right]^2, \quad (1)$$

where a is the absorption coefficient, h is the sample thickness, R is the reflection coefficient, which depends on the wavelength, T is the linear light transmission coefficient, n_1 and n_2 are the refractive indices of the input and output media [19].

The chemical analysis of the sulfur and selenium concentrations in the ZnS_xSe_{1-x} bulk crystals was performed by atomic spectroscopy with inductively coupled plasma spectroscopy. For optical studies, an optical emission spectrometer CAP 6300 Duo (Thermo Scientific, USA) was used. The measurement limit and the measurement accuracy were 10^{-1} – 10^{-5} mass.% and up to 0.5% of the measured value, respectively.

3. Results

The value of the optical band gap was estimated from the optical transmittance spectra. The transmission studies were carried out at room temperature for a large number of the ZnS_xSe_{1-x} single crystals with different values of x . The thicknesses of the samples were equal to 4 mm. Near-ultraviolet, visible, and near-infrared transmission spectra of ZnS_xSe_{1-x} single crystals are shown in Fig. 1. The transmittance values of ZnS_xSe_{1-x} bulk crystals were equal to 67% for ZnS_{0.39}Se_{0.61} and ZnS_{0.07}Se_{0.93} ones (at $\lambda = 1100$ nm). This fact indicates a high crystalline quality of our crystals.

The optical loss coefficient was calculated according to Eq. (1) and was used for the calculation of the direct and indirect transitions [20, 21]. The band gap value was determined from the transmission spectra. Both direct and indirect optical transitions are possible. Direct transitions give rise to:

$$a \approx (E_{pt} - E_g)^{1/2}, \quad (2)$$

where E_g is the vertical separation between the valence and conduction bands, and E_{pt} is the photon energy [20].

Figure 2 shows the plot of a_2 versus the photon energy. If the linear parts are extrapolated to the zero absorption coefficient, the indicated values for the direct transitions [20] are lying between 2.59 and

2.78 eV for $\text{ZnS}_x\text{Se}_{1-x}$ samples, where $x = 0.07-0.39$. Direct energy transitions for $\text{ZnS}_{0.07}\text{Se}_{0.93}$ and $\text{ZnS}_{0.39}\text{Se}_{0.61}$ are 2.59 ± 0.01 and 2.78 ± 0.01 eV, respectively (see Table). Indirect transitions can be written as:

$$a \approx (E_{\text{pt}} - E_g + E_{\text{ph}})^2, \quad (3)$$

where E_{ph} is the phonon energy [21].

Figure 3 shows a plot of $a^{1/2}$ versus the photon energy. The extrapolation of linear parts to the zero absorption coefficient gives the values for indirect transitions equal to 2.49 ± 0.01 and 2.70 ± 0.01 for $\text{ZnS}_{0.07}\text{Se}_{0.93}$ and $\text{ZnS}_{0.39}\text{Se}_{0.61}$, respectively (see Table). The transmission spectra were measured five times in different parts of the crystal. According to these spectra, the error of measurements of the direct and indirect transitions is not larger than 0.01 eV. The direct (E_{g1}) and indirect (E_{g2}) transitions of the $\text{ZnS}_x\text{Se}_{1-x}$ bulk crystals are shown in Table.

An increase of the sulfur concentration leads to an increase of the band gap energy for both direct (Fig. 2) and indirect (Fig. 3) transitions. The dependence of the band gap on the concentrations of sulfur was fitted by Eq. (4) with b as a variable parameter [22]. The resulting curves are shown in Fig. 4. Here, $E_g(x)$ is a continuous function of x . The last was obtained by a chemical analysis

$$E_g(x) \approx x E_A + (1-x) E_B - b x (1-x), \quad (4)$$

where x is the concentration of S, E_A is the energy gap of pure ZnS, E_B is the energy gap of pure ZnSe, and b is the bowing coefficient.

The optical bowing parameters b for $\text{ZnS}_x\text{Se}_{1-x}$ bulk crystal are equal to 0.1 falling into the range of the reported optical bowing parameters (0–0.63) [3, 23–26]. The energy of the band gap for pure ZnS and ZnSe compounds was calculated by means of Eq. (4). The indirect transitions for ZnS and ZnSe compounds are equal to 3.17 eV and 2.43 eV, and the direct transitions are 3.22 eV and 2.54 eV, respectively, according to

$$E_g(x) \approx x E_A + (1-x) E_B - b x (1-x). \quad (5)$$

4. Discussion

The optical band gap change of bulk $\text{ZnS}_x\text{Se}_{1-x}$ semiconductors ($x = 0.07-0.39$) obtained by the direc-

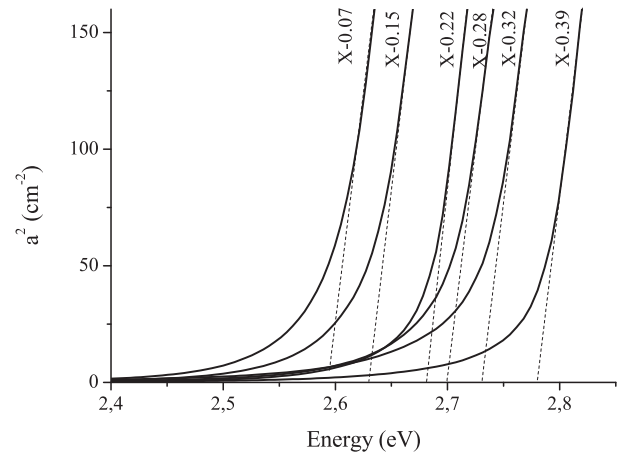


Fig. 2. Plot of the absorption coefficient squared versus the photon energy for $\text{ZnS}_{0.07}\text{Se}_{0.93}$ (a), $\text{ZnS}_{0.15}\text{Se}_{0.85}$ (b), $\text{ZnS}_{0.22}\text{Se}_{0.78}$ (c), $\text{ZnS}_{0.28}\text{Se}_{0.72}$ (d), $\text{ZnS}_{0.32}\text{Se}_{0.68}$ (e), $\text{ZnS}_{0.39}\text{Se}_{0.61}$ (f) crystals

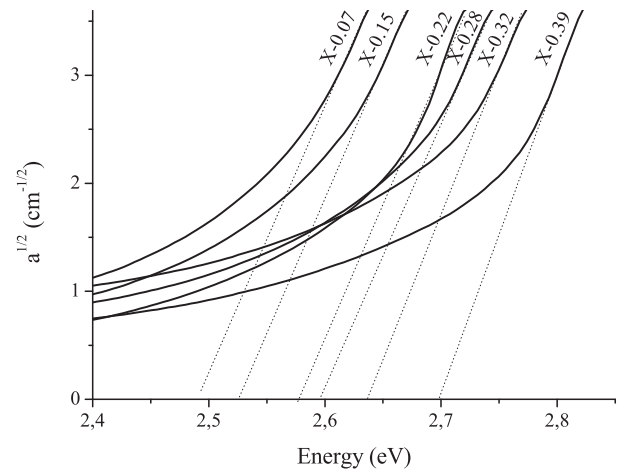


Fig. 3. Plot of the absorption coefficient root versus the photon energy for $\text{ZnS}_{0.07}\text{Se}_{0.93}$ (a), $\text{ZnS}_{0.15}\text{Se}_{0.85}$ (b), $\text{ZnS}_{0.22}\text{Se}_{0.78}$ (c), $\text{ZnS}_{0.28}\text{Se}_{0.72}$ (d), $\text{ZnS}_{0.32}\text{Se}_{0.68}$ (e), $\text{ZnS}_{0.39}\text{Se}_{0.61}$ (f) crystals

Direct (E_{g1}) and indirect (E_{g2}) transitions of the $\text{ZnS}_x\text{Se}_{1-x}$ bulk crystals

Compounds	E_{g1} , eV	E_{g2} , eV
$\text{ZnS}_{0.07}\text{Se}_{0.93}$	2.59	2.49
$\text{ZnS}_{0.15}\text{Se}_{0.85}$	2.63	2.57
$\text{ZnS}_{0.22}\text{Se}_{0.78}$	2.68	2.58
$\text{ZnS}_{0.28}\text{Se}_{0.72}$	2.70	2.60
$\text{ZnS}_{0.32}\text{Se}_{0.68}$	2.73	2.64
$\text{ZnS}_{0.39}\text{Se}_{0.61}$	2.78	2.70

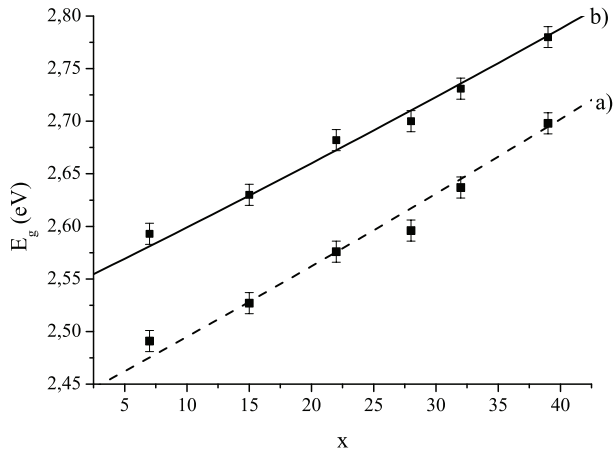


Fig. 4. Dependence of the band gap energy (eV) on the concentration of sulfur for indirect (a) and direct (b) transitions for the $\text{ZnS}_x\text{Se}_{1-x}$ bulk crystal, where $x = 0.07-0.39$. The points indicate the experimental results, the solid and dash straight lines represent the dependences calculated according to Eq. (4)

tional solidification method is investigated. The calculated values of the optical band gaps for ZnS and ZnSe are 3.22 eV and 2.54 eV, respectively, which is close to the values reported for the bulk crystals (3.54 and 2.58 eV, respectively) [27, 28]. The estimated too small value of the energy gap of ZnS is probably caused by the not correct estimation of the bowing parameter due to the lack of experimental data for large S contents in the crystal.

In a normal isovalent $\text{AB}_x\text{C}_{1-x}$ crystal, an increase of x leads to the moving of the conduction and valence bands, and no new (defect) levels appear in the band gap. The continuous change of the band gap of the $\text{ZnS}_x\text{Se}_{1-x}$ crystals with the composition indicates the normal isovalent formation of crystals grown by the directional solidification. The high optical quality and smooth dependence of the optical band gap on the composition indicate a possibility of growing $\text{ZnS}_x\text{Se}_{1-x}$ crystal by directional solidification techniques for x-ray and γ -ray detectors.

The wider band gap and higher atomic mass ratio of $\text{ZnS}_x\text{Se}_{1-x}$ as compared to ZnSe(Te) or/and ZnSe(Al) crystals extend application areas of such semiconductors. In addition, this may offer a completely different new type of x-ray and γ -ray detectors based on $\text{ZnS}_x\text{Se}_{1-x}$ bulk crystals. However, it should be noted that knowledge about the energy gap is not sufficient for the development of x-ray and

γ -ray detectors based on $\text{ZnS}_x\text{Se}_{1-x}$, and other investigations are required. Therefore, the further work should involve: luminescence properties, light output, afterglow and kinetic parameters of $\text{ZnS}_x\text{Se}_{1-x}$ bulk crystal.

5. Conclusion

The band gap and optical properties of $\text{ZnS}_x\text{Se}_{1-x}$ bulk crystal have been analyzed as functions of the sulfur concentration. A change of the sulfur content does not lead to the appearance of new states or defects, and the band gap is changed continuously with the composition. Good optical properties and the smooth composition dependence of the optical band gap of $\text{ZnS}_x\text{Se}_{1-x}$ bulk crystals grown by the directional solidification techniques indicate a possibility of the development of $\text{ZnS}_x\text{Se}_{1-x}$ -based x-ray and γ -ray detectors.

The authors thank Alexander Shkurmanov (Felix Bloch Institute for Solid State Physics, Universität Leipzig) for discussions.

1. M. Emam-Ismael, M. El-Hagary, E. Ramadan *et al.* Influence of γ -irradiation on optical parameters of electron beam evaporated $\text{ZnSe}_{1-x}\text{Te}_x$ nanocrystalline thin films. *Radiat Eff. Defects Solids.* **169** (1), 61 (2014).
2. P. Shotanus, P. Dorenbos, V. Ryzhikov. Detection of CdS (Te) and ZnSe (Te) scintillation light with silicon photodiodes. *IEEE Trans. Nucl. Sci.* **39** (4), 546 (1992).
3. T. Homann, U. Hotje, M. Binnewies *et al.* Composition-dependent band gap in $\text{ZnS}_x\text{Se}_{1-x}$ a combined experimental and theoretical study. *Solid State Sci.* **8** (1), 44 (2006).
4. L.S. Lai, I.K. Sou, C.W. Law *et al.* ZnSSe-based ultraviolet photodiodes with extremely high detectivity. *Opt. Mater.* **23** (1), 21 (2003).
5. G. Kudlek, N. Presser, J. Gutowski *et al.* Comparative optical investigations of ZnSe/GaAs epilayers grown by molecular beam and hot-wall epitaxy. *J. Appl. Phys.* **68** (11), 5630 (1990).
6. C.T. Hsu. Growth of $\text{ZnS}_x\text{Se}_{1-x}$ layers on Si substrates by atomic layer epitaxy. *Mater. Chem. Phys.* **58** (1), 6 (1999).
7. J.H. Song, E.D. Sim, K.S. Baek *et al.* Optical properties of $\text{ZnS}_x\text{Se}_{1-x}$ ($x < 0.18$) random and ordered alloys grown by metalorganic atomic layer epitaxy. *J. Cryst. Growth.* **214**, 460 (2000).
8. P. Prete, N. Lovergine, S. Petroni *et al.* Functional validation of novel Se and S alkyl precursors for the low temperature pyrolytic MOVPE growth of ZnSe, ZnS and ZnSSe. *Mater. Chem. Phys.* **66** (2) (2000).
9. M. Ambrico, G. Perna, D. Smaldone *et al.* Structural and optical parameters of films deposited on quartz substrates

- by laser ablation. *Semicond. Sci. Technol.* **13** (12), 1446 (1998).
10. L. Atroshchenko, L. Gal'chinetskii, S. Galkin *et al.* Structure defects and phase transition in tellurium-doped ZnSe crystals. *J. Cryst. Growth.* **198**, 292 (1999).
 11. L. Atroshchenko, L. Gal'chinetskii, S. Galkin *et al.* Influence of the growth parameters and subsequent annealing upon structural perfectness, optical and mechanical properties of $ZnSe_{1-x}Te_x$ crystals. *Func. Mat.* **8** (3), 455 (2001).
 12. R. Hussein, O. Pages, F. Firszt *et al.* Near-forward Raman study of a phonon-polariton reinforcement regime in the Zn(Se,S) alloy. *J. Appl. Phys.* **116** (8), 1 (2014).
 13. R. Hussein, O. Pages, S. Doyen-Schuler *et al.* Percolation-type multi-phonon pattern of Zn(Se,S): Backward/forward Raman scattering and ab initio calculations. *J. Alloys Compd.* **644**, 704 (2015).
 14. R. Hussein, O. Pages, A. Polian *et al.* Pressure-induced phonon freezing in the ZnSeS II–VI mixed crystal: phonon-polaritons and ab initio calculations. *J. Phys. Condens. Matter.* **28** (20), 5401 (2016).
 15. S. Venkatachalam, D. Mangalaraj, S. Narayandass *et al.* The effect of nitrogen ion implantation on the structural, optical and electrical properties of ZnSe thin films. *Semicond. Sci. Tech.* **21** (12), 1661 (2006).
 16. Y. Chen, J. Li, X. Yang *et al.* Band gap modulation of the IV, III–V, and II–VI semiconductors by controlling the solid size and dimension and the temperature of operation. *J. Phys. Chem. C.* **115** (47), 23338 (2011).
 17. Y. Alghamdi. Composition and band gap controlled AACVD of ZnSe and ZnS_xSe_{1-x} thin films using novel single source precursors *Mat. Sci. Appl.* **8** (10), 726 (2017).
 18. B. Pejova, B. Abay, L. Bineva *et al.* Temperature dependence of the band-gap energy and sub-band-gap absorption tails in strongly quantized ZnSe nanocrystals deposited as thin films. *J. Phys. Chem. C.* **114** (36), 15280 (2010).
 19. D.B. Judd. Fresnel reflection of diffusely incident light. *J. Res. Natl. Bur. Stand.* **29** (5), 329 (1942).
 20. R.H. Bube. *Photoconductivity of Solids* (Wiley, 1960).
 21. R. Summitt, J.A. Marley, N.F. Borrelli *et al.* The ultraviolet absorption edge of stannic oxide (SnO_2). *J. Phys. Chem. Solids.* **25** (12), 1465 (1964).
 22. J.E. Bernard, A. Zunger, Electronic structure of ZnS, ZnSe, ZnTe, and their pseudobinary alloys. *Phys. Rev. B* **36** (6), 3199 (1987).
 23. A.A. El-Shazly, M.M. El-Naby, M.A. Kenawy *et al.* Optical properties of ternary ZnS_xSe_{1-x} polycrystalline thin films. *Natl. Bur. Stand.* **36** (1), 51 (1985).
 24. S. Larach, R.E. Shrader, C.F. Stocker. Anomalous variation of band gap with composition in zinc sulfo- and selenotellurides. *Phys. Rev.* **108** (3), 587 (1957).
 25. A. Ebina, E. Fukunaga, T. Takahashi. Variation with composition of the E_0 and $E_0 + \Delta_0$ gaps in ZnS_xSe_{1-x} alloys. *Phys. Rev. B* **10** (6), 2495 (1974).
 26. L.G. Suslina, D.L. Fedorov, S.G. Konnikov *et al.* Dependence of forbidden-band width on composition of ZnS_xSe_{1-x} mixed-crystals. *Sov. Phys. Semicond.* **11** (10), 1132 (1997).
 27. A.V. Novoselova, V.B. Lazarev (Eds.). *Physical and Chemical Properties of Semiconductors* (Nauka, 1979) (in Russian).
 28. P. Herve, L.K. Vandamme. General relation between refractive index and energy gap in semiconductors. *Infrared Phys. Technol.* **35** (4), 609 (1994).

Received 08.09.17

О.Г. Трубаєва, О.І. Лалаянц, М.А. Чайка

ЗМІНА ЗАБОРОНЕНОЇ ЗОНИ ZnS_xSe_{1-x}
ОБ'ЄМНИХ НАПІВПРОВІДНИКІВ ШЛЯХОМ
РЕГУЛЮВАННЯ ВМІСТУ СІРКИ

Резюме

Об'ємні кристали ZnS_xSe_{1-x} були вирощені за методом Бриджмена–Стокбаргера. Прозорість зразків ZnS_xSe_{1-x} становила від 67% до 56% на $\lambda = 1100$ нм (товщина зразка 4 мм), що вказує на високу оптичну якість кристалів. Оптичні експерименти показали відсутність нових станів з включенням сірки, заборонена зона безперервно рухається зі складом. Оптична ширина забороненої зони ZnS_xSe_{1-x} кристала варіювалася від 2,59 до 2,78 еВ для прямих переходів і від 2,49 до 2,70 еВ для непрямих переходів